

# Structural Matching between the Polymeric Nucleating Agent Isotactic Poly(vinylcyclohexane) and Isotactic Polypropylene

Daniel Alcazar, Jrjeng Ruan,<sup>†</sup> Annette Thierry, and Bernard Lotz\*

Institut Charles Sadron (CNRS-ULP), 6, rue Boussingault, 67083 Strasbourg, France

Received December 12, 2005; Revised Manuscript Received January 24, 2006

**ABSTRACT:** Poly(vinylcyclohexane) (PVCH) is a patented polymeric nucleating agent for isotactic polypropylene (iPP) and induces its  $\alpha$  crystal modification ( $\alpha$ iPP). The structural interactions at the root of this activity are investigated by analyzing the transcrystallization of single crystals of  $\alpha$ iPP on single crystals of PVCH. Electron microscopy results indicate (i) a quasi-perfect two-dimensional lattice match in the contact plane, with (100)<sub>PVCH</sub> facing (110) <sub>$\alpha$ iPP</sub> or ( $\bar{1}10$ ) <sub>$\alpha$ iPP</sub> planes, and (ii) a consistent link between the PVCH single crystals' internal structure and the orientation of  $\alpha$ iPP overgrowth. The two polymers chain axes are parallel. The 3-fold (iPP) and 4-fold (PVCH) helices share the same chain axis repeat ( $\approx 6.5$  Å), and repeat distances normal to the chain axis are  $\approx 21.9$  Å for (110) <sub>$\alpha$ iPP</sub> and (100)<sub>PVCH</sub> planes. In chain axis projection, the PVCH helices are tilted relative to the  $a$  and  $b$  axes of the tetragonal unit cell. The tilt generates an "asymmetric sawtooth" surface profile that differs for clock- or counterclockwise tilts. Similar surface profiles exist in the (110) <sub>$\alpha$ iPP</sub> or ( $\bar{1}10$ ) <sub>$\alpha$ iPP</sub> contact planes. Matching of the PVCH and iPP sawteeth profiles is selective and induces a single orientation of the  $\alpha$ iPP crystal lattice in the overgrowth. The orientation of the  $\alpha$ iPP overgrowth thus becomes also a marker of the local clock- or counterclockwise setting of PVCH helices in the growth face.

## Introduction

Epitaxial crystallization between a polymer and low-molecular-weight materials that act as nucleating agents (NA) is well documented.<sup>1,2</sup> Relatively few examples of interactions between a crystalline polymer and another crystalline polymer acting as a nucleating agent have been analyzed. An early report<sup>3</sup> describes the mutual nucleating activity of polyethylene (PE) toward isotactic polypropylene (iPP) depending on the thermal treatment applied. Some interactions have been characterized at a structural level: polyamides/iPP,<sup>4</sup> the mutual activity of iPP and PE,<sup>5</sup> and poly(tetrafluoroethylene) (PTFE)/iPP.<sup>6</sup> The interactions rest on different types of epitaxial interactions in which either the interchain distances or, in the case of helical polymers, the interstrand distances are involved.<sup>7</sup>

Polymeric nucleating agents (PNA) are presently considered as a class of nucleating agents on its own<sup>8</sup> and have reached the production line. The high melting ( $T_m > 400$  °C) polyolefin isotactic poly(vinylcyclohexane) (PVCH) is used to nucleate iPP in its  $\alpha$  form ( $\alpha$ iPP).<sup>9</sup> Initially, PVCH was selected by Kakugo et al.<sup>10</sup> as a potential nucleating agent "because (they) thought that polymers to act as a nucleation agent should be crystalline at the crystallization temperature of iPP". (Note, however, that this condition is also explicit in the earlier<sup>3</sup> thermal treatments used to illustrate the PE/iPP mutual nucleating activity.) Kakugo et al. indicate a very high efficiency even at concentrations down to  $10^{-2}$  wt ppm. However, the mechanism by which PVCH and iPP interact is still not known. It is tempting to consider that dimensional match of the two chain axis repeat distances is involved. The  $c$  parameters of the unit cells are very close: 6.43 Å<sup>11</sup> and 6.5 Å, respectively. However, PVCH and iPP have different helical conformations, with four and three residues per turn, respectively.<sup>12</sup>

In the present report, we investigate in detail the structural relationship at the root of the nucleating activity of PVCH

toward iPP. This study is a continuation of our investigation of the structure of single crystals of PVCH. It helped to show that solution-grown single crystals are polysynthetic twins.<sup>13</sup> The investigation technique differs in one important respect from earlier investigations in this laboratory. The previous investigations relied for the most part on successive epitaxial crystallizations, thus generating polymer films with the chain axis in the plane of the film.<sup>1</sup> In the present case, melt-grown single crystals of the nucleating agent are found to be more appropriate. The lateral edges of the PVCH crystals act as a substrate for the transcrystalline growth of single crystals of  $\alpha$ iPP. This approach helps determine the facing planes involved in the interaction (via composite  $hk0$  diffraction patterns) and reveals an unexpected dependence of the iPP growth direction ( $a^*$ -axis orientation) on the internal structure of PVCH, namely on the azimuthal setting of the PVCH helices in the crystal lattice. It establishes a two-dimensional match, and more importantly, it demonstrates that a definite topographic match is at play between the nucleating (PVCH) and nucleated ( $\alpha$ iPP) polymeric species.

## Experimental Section

**Sample and Preparation Methods.** The sample of PVCH was the same sample provided by Sumitomo Chemical Co. Ltd. as used in a previous study from this laboratory.<sup>13</sup> Its molecular weight is about  $2.4 \times 10^5$ .

As developed in our previous report, the preparation of suitable single crystals of PVCH was performed via solution-assisted melt crystallization of thin films. The films are not of uniform thickness but display relatively large domains with dense populations of PVCH monolamellar crystals highly suited for our investigation.

Deposition from solution of iPP on single crystals of PVCH is difficult. PVCH crystals, despite their high melting temperature, tend to dissolve in the hot solvents used to spread iPP. To alleviate this difficulty, a vapor deposition process was mostly used. A small amount of iPP ( $\approx 1$  mg) is placed in a molybdenum crucible and heated under vacuum (to about 300 °C) in a bell jar. The iPP is partially degraded and vaporizes. The vapors deposit and condense on microscope cover slides with PVCH single crystals mounted

<sup>†</sup> Present address: Institute of Materials Science and Engineering, National Sun Yat-sen University, Kaohsiung 804, Taiwan, ROC.

\* Corresponding author: e-mail lotz@ics.u-strasbg.fr.

some  $\approx 10$  cm above the crucible. The procedure has one advantage and one drawback. On one hand, the iPP deposit is of uniform thickness, a thickness that can be further controlled by adjusting the amount of iPP that is vaporized. On the other hand, the major drawback is that the vaporized iPP has a relatively low molecular weight ( $\approx 3000$ ). As a result, a significant fraction of  $\gamma$  phase is produced upon iPP crystallization. This drawback is however of limited consequences when it comes to analyzing the PVCH/ $\alpha$ iPP structural relationship. Indeed, for these vaporized low-MW iPPs, the higher-MW fraction crystallizes first in the  $\alpha$ iPP modification of interest. Epitaxial crystallization of the  $\gamma$  phase on this  $\alpha$  phase takes place only in a second stage. Furthermore, the structural relationship between the two phases is well-documented.<sup>12,14</sup> In the following, the  $\gamma$  phase will not be further mentioned beyond noting in some diffraction patterns the presence of its characteristic reflection (spacing  $4.45 \text{ \AA}^{-1}$ , indexed as 117 in the orthorhombic unit cell with nonparallel chain axes due to Brückner and Meille).<sup>15</sup> The analysis of the epitaxial interactions will concentrate on the  $\alpha$  phase, since the presence of the  $\gamma$  phase is merely a side effect linked with the conditions used to deposit the iPP layer. Anticipating results to come, this statement is further supported by the fact that the observed contact plane is specific to  $\alpha$ iPP and does not make physical sense for the  $\gamma$  phase.

The thermal treatments were carried out under a blanket of nitrogen in a Linkam 600 hot stage. For electron microscopy observations, the samples are shadowed with Pt when desired and coated with a carbon film. As is usually observed after a prolonged stay of glass slides at high temperature, the polymer tends to stick to the glass, and detachment of the crystals from the glass support is difficult. The standard detachment technique using poly(acrylic acid) as a backing was not satisfactory: most of PVCH single crystals remained stuck on the glass slides, whereas only small fragments went off with the carbon film and iPP sample. Since we had to investigate the structural relationship at a local scale, namely at the PVCH crystal edges, we resorted to dissolution of the glass support slides by hydrofluorhydric acid: this procedure preserved the PVCH crystals.

**Investigation Techniques.** Observation of the crystal morphology and selection of suitable samples for electron microscopy was performed under phase contrast with Leitz and Zeiss optical microscopes. Electron microscopic examination was performed with a Philips CM12 operated at 120 kV. As a rule, the sample was scanned at low magnification ( $\approx 1000$ ) using the defocused diffraction pattern mode. Bright field images, diffraction patterns, and dark-fields were recorded with a MegaView III digital camera (Soft Imaging System) and/or on photographic plates (Kodak SO163, developed with undiluted D19 for 12 min). In the latter case, dark-field images could be recorded at a direct magnification of 3000 on the photographic plates. Molecular modeling and diffraction pattern calculation were performed with the appropriate modules of the Cerius<sup>2</sup> program developed by Accelrys.

### Background: Topographical Features of PVCH and $\alpha$ iPP Crystal Structures

The structural relationships to be established in this article turn out to involve rather complex topographies of the contact planes. Anticipating later results, these are the (100)<sub>PVCH</sub> and (110) <sub>$\alpha$ iPP</sub> or (110) <sub>$\alpha$ iPP</sub> planes. The crystal structures and the contact faces' topographical features are first described to ease later analyses. In this description, the possibility of up-down disorder is not taken into account since it does not feature in the analysis of the epitaxies. Indeed, the shape of anticline helices is nearly similar, which does not affect much the contact face topography.

**Structure of PVCH Form I.** PVCH is a high melting polyolefin that owes many of its properties to the fact that ramification takes place in the  $\alpha$ -position of the (bulky) side chain. Similar high melting temperatures are observed for e.g. isotactic poly(3-methyl-1-butene).

Two crystal structures are known for PVCH. Form II is obtained at high temperature under stress and has a 24<sub>7</sub> helix geometry. The stable crystal modification form I of interest in the present investigation has a tetragonal unit cell with parameters  $a = b = 21.99 \text{ \AA}$ ,  $c = 6.43 \text{ \AA}$ .<sup>11</sup> The cell contains four helices with 4-fold symmetry: two right-handed 4<sub>1</sub> and two left-handed 4<sub>3</sub> helices. De Rosa et al. determined the space group of the cell to be  $I4_1/a$ .<sup>16</sup> Some specific features of this space group are fundamental in the frame of the present investigation. Indeed, the  $I4_1/a$  symmetry is characterized by the fact that, in  $c$ -axis projection, the helices are slightly rotated relative to the cell edges (Figure 1a). As a result of this rotation, the (010) and (100) lateral cell surfaces (and crystal growth faces) are not flat, but rather corrugated. Furthermore, the corrugation is not symmetric: it depends on the clock- or counterclockwise rotation of the helices on their axes (Figure 1a). For this reason, the contact faces will be described in this paper as having an "asymmetric sawteeth" profile.

The possibility of clock- or counterclockwise rotation of helices in the unit cell is at the root of twinning by merohedry. As analyzed in detail in our previous work, single crystals are often twins, with twin components differing by the azimuthal setting of the chains. This is reflected, on their outer surface, by the orientation of the corrugations as observed in  $c$ -axis projection (cf. later, Figure 1c top). Crystals grown from squalane or phenyldecane solutions are even polysynthetic twins.<sup>13</sup> The twinned components can be differentiated in dark-field electron microscopy by taking advantage of the asymmetry (or "handedness") of the diffraction pattern (Figure 1b). In twins by merohedry, different reflections overlap. This holds true for example for the strong 240<sub>ccw</sub> spot of parts of the crystal and the weak 240<sub>cw</sub> spot of the rest of the crystal in twin relationship (in the following, cw and ccw indices stand for clock- and counterclockwise rotation of the PVCH helices, respectively). By selecting this overlapped reflection and imaging the crystal in dark-field, those parts of the crystal contributing to the strong 240<sub>ccw</sub> show up as bright domains, whereas the twinned areas, imaged through the weaker 240<sub>cw</sub> spot, are significantly darker (cf. later, Figure 7). Pradère et al.<sup>17</sup> pioneered this specific use of dark-field imaging on single crystals of isotactic poly(4-methyl-1-pentene) in its form III, a crystal modification that displays the same cell geometry and symmetry as PVCH.

Apart from the corrugation of the surface topography considered so far (Figure 1), the (100) plane of PVCH also displays two additional, symmetrical and equivalent corrugations that are tilted to the chain axis. This feature is best illustrated when the outer, most exposed CH<sub>2</sub> groups of the cyclohexyl rings are highlighted, as shown in Figure 1c. Curiously, although the helices are right- and left-handed with 4-fold symmetry, the outer features are roughly  $c/2$  apart in the contact plane, which mimics a 2<sub>1</sub> helical symmetry in that contact plane. The outer CH<sub>2</sub> groups of neighbor helices are furthermore nearly aligned and therefore form linear gratings that highlight the intersection of the {021} planes with the (100) contact plane and are oriented at some 57° to the chain axis direction. Expectedly, since both right-handed and left-handed helices build up the contact plane, the two symmetric orientations at +57° and -57° to the chain axis are equivalent (underlined in Figure 1c). The (100) planes of PVCH are therefore racemic from both helix chirality (existence of helices of both hands) and topographical<sup>18</sup> standpoints. This peculiarity will become an important ingredient in the analysis of the epitaxial relationship.

To summarize, the (100) contact face of PVCH is characterized by two features: the "asymmetric sawteeth pattern" when

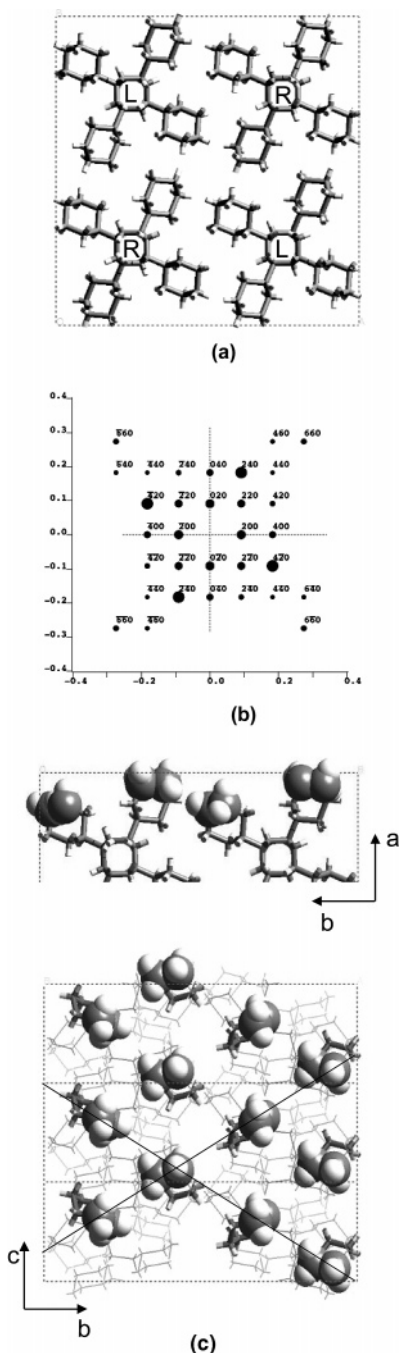


**Figure 1.** (a) Crystal structure of PVCH form I, as determined by De Rosa et al.<sup>16</sup> Two right-handed and two left-handed helices per cell, space group  $I4_1/a$ . The setting of helices is counterclockwise. (b) Calculated diffraction pattern of PVCH showing the asymmetry generated by the rotation of the helices relative to the cell edges. Note that the sense of the swastika  $420-220-020-020-220-420$  is also counterclockwise. (c) Organization of the exposed cyclohexyl groups in the lateral (100) or (010) faces. The exposed  $\text{CH}_2$  groups are highlighted (represented as balls). Views along the  $c$  axis (top) and normal to this plane (in the bottom figure, three unit cells are shown). Note that the exposed groups are aligned nearly parallel to the  $(021)$  and  $(0\bar{2}1)$  planes (underlined). They are  $5.5 \text{ \AA}$  apart and tilted some  $57^\circ-60^\circ$  relative to the chain axis. The lateral faces of the helices therefore mimic a 2-fold helical symmetry although the helix has 4-fold symmetry, which adds to their racemic topographical character.

seen in chain axis projection and the existence of rows of cyclohexyl groups edges that form two symmetric rows at  $57^\circ$  to the chain axis.

**Structure of Isotactic Polypropylene,  $\alpha$  Form.** The structure of  $\alpha$ iPP is well-known, but the topography of the planes

involved in epitaxial relationships is less familiar. Two crystallographic planes have been observed to be contact planes in previously reported epitaxial crystallization: the (010) and (110) planes. The (010) plane (more specifically, the (010) plane that contains the least methyl groups; cf. Figure 2a) is a contact plane in the epitaxy of iPP with many nucleating agents (e.g., sodium benzoate). It is also involved in the homoepitaxy at the root of the lamellar branching of  $\alpha$ iPP<sup>4</sup> and in the nonparallelism of chain axes characteristic of the  $\gamma$  form unit cell.<sup>15</sup> Its surface structure is a quasi-perfect lozenge array of protruding methyl groups parallel to the  $[101]$ ,  $[\bar{1}01]$ , and  $[001]$  directions, with inter-row distances of  $4.25$ ,  $5.05$ , and  $6.55 \text{ \AA}$ , respectively.

The (110) contact plane has been observed less frequently than the (010) contact plane. It features in the epitaxy of  $\alpha$ iPP on PTFE and on some organic acids or their salts. In all cases analyzed so far, the substrates display rows of prominent features  $5.5 \text{ \AA}$  apart: rows of chlorine atoms on the surface of  $p$ -chlorobenzoic acid crystals<sup>7</sup> or interhelix distance in PTFE friction-deposited layers.<sup>6</sup> The surface topography of the (110) plane is more complex than the (010) one since the plane intersects at a  $73^\circ$  angle to the  $a$  axis the familiar  $\alpha$ iPP  $ac$  layers. This (110) plane is made of alternating right- and left-handed helices (Figure 2a).

Interestingly, the surface topography of the  $(110)_{\alpha\text{iPP}}$  plane also reveals two structural features very similar to those described for PVCH. These are best understood by referring to Figure 2c which represents  $c$ -axis projections and normal projections (along directions indicated by the arrows) of the two possible contact faces for both  $(110)_{\alpha\text{iPP}}$  and  $(\bar{1}\bar{1}0)_{\alpha\text{iPP}}$ .

First, when observed normal to the chain axis, the plane displays rows of methyl groups  $5.5 \text{ \AA}$  apart that are tilted at some  $57^\circ$  to the iPP chain axes (highlighted by thin lines in the four center projections of Figure 2c). Contrary to PVCH, however, the right- and left-handed helices do not play similar roles in any one contact face. For a given layer, only one direction (parallel either to  $[112]$  or  $[\bar{1}\bar{1}2]$ ) is highlighted, which corresponds roughly to the orientation of the outer path of the most exposed helices. Symmetrical tilt angles (at  $+57^\circ$  and  $-57^\circ$  to the chain axis) do exist for helices of opposite hand, but they are found on opposite sides (i.e., as seen from  $+a$  or  $-a$ ) of any one layer ( $(110)$  and  $(\bar{1}\bar{1}0)$ ). In Figure 2c, the top right and bottom left contact faces display a “right-handed tilt” of the methyl rows, and the bottom right and top left contact faces display a “left-handed” tilt of the methyl rows. As described in an earlier work, these rows of methyl groups may become oriented parallel to a linear grating (say a substrate made of parallel PTFE helices). When analyzing epitaxial relationships of this type, the  $+57^\circ$  or  $-57^\circ$  tilt of the iPP chain axis relative to the substrate grating orientation helps discriminate between the right- or left-helical hand of the iPP helices that build up the contact plane—a rare insight into structural analysis of polymers.<sup>6</sup>

The second topographical feature of the  $(110)_{\alpha\text{iPP}}$  plane has not been taken into account in previous structural analyses of  $\alpha$ iPP epitaxy but will feature prominently in the present work. When seen along the chain axis, the (110) face is not flat (outer parts in Figure 2c,  $c$ -axis projections). It intersects 3-fold helices that have one of their “faces” oriented parallel to the  $ac$  plane and their two other faces at  $\pm 30^\circ$  to the  $b$  axis. The surface topography of the  $(110)_{\alpha\text{iPP}}$  plane thus presents a periodic “buckling” or “corrugation” with  $\approx 11 \text{ \AA}$  periodicity. The longer part of the corrugation is, again, parallel to the face of the most exposed helix in the contact face (Figure 2c). As for PVCH,



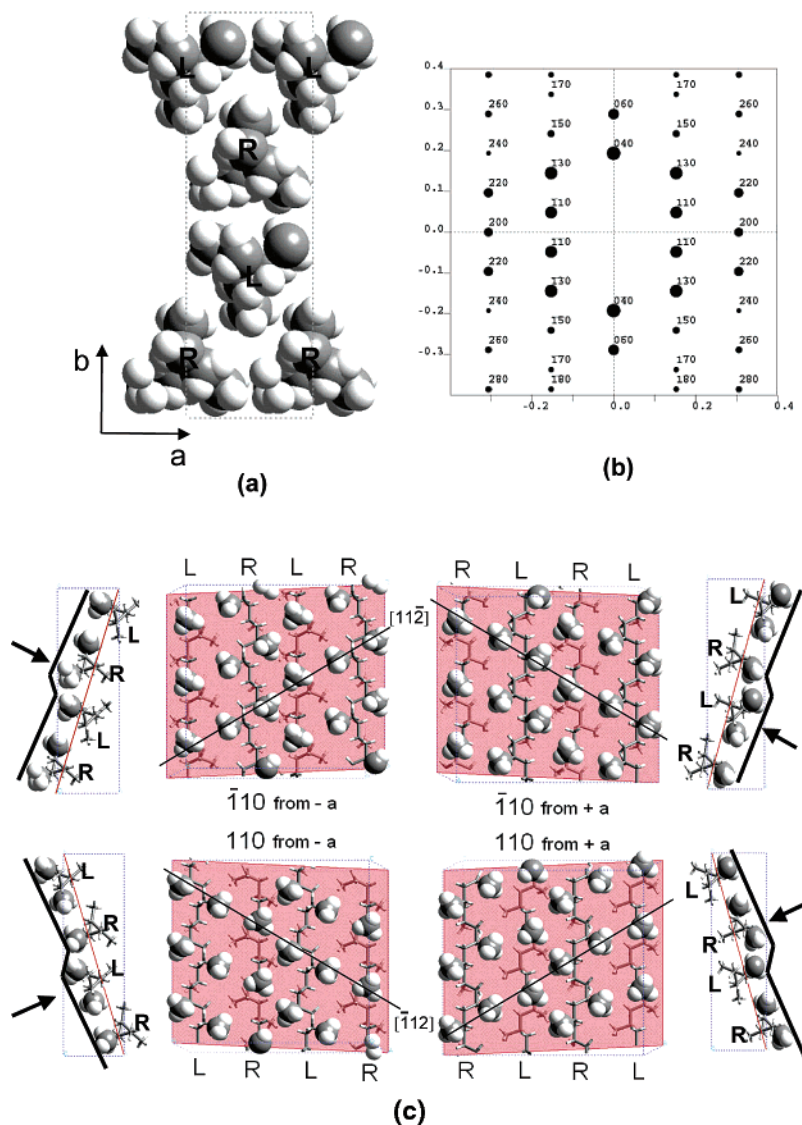


**Figure 2.** (a) Crystal structure of iPP,  $\alpha$  form, as seen in chain axis projection. The cell symmetry is shown here as  $Cc$ . (b) Simulated  $hk0$  diffraction pattern of  $\alpha$ iPP. (c) Chain axis projections and topography of the  $\alpha$ iPP (110) and  $(\bar{1}10)$  layers and contact faces. The hand of helices is indicated. Note that the asymmetric sawteeth pattern in chain axis projection (underlined by thick lines, outer models) is identical for the front and back faces of any one layer. It differs for the (110) (top) or  $(\bar{1}10)$  (bottom) layer. The tilt of the rows of methyl groups (inner models) is underlined with thinner lines.

the corrugation is asymmetric, which means that two “orientations” of the corrugations are possible (in the following, these corrugations will be referred to also as “asymmetric sawteeth”). Note, however, that the orientation of the asymmetry is now different for the (110) layer and the  $(\bar{1}10)$  layer and does not depend on the sense of observation ( $+a$  or  $-a$ ). Referring to Figure 2c, the top part shows the  $(\bar{1}10)$  layer. In the outer  $c$ -axis projections, the arrows point to the two surfaces, highlighted by the thick lines. From the perspective of the arrows, these surfaces have a step, with the higher step located to the left of the arrows. The situation is reversed for the (110) layer (bottom part of Figure 2c): the higher part is on the right and the lower part on the left of the arrow.

To summarize, the four possible contact faces of  $\alpha$ iPP have two major topographical features: rows of methyl groups and an asymmetric sawtooth profile (in  $c$ -axis projection, i.e., when the contact face is seen edge-on). The rows of methyl groups define a chirality for each contact face; opposite sides of a given (110) layer have opposite chiralities (to be contrasted with PVCH that is, in this respect, racemic). Two asymmetric sawtooth profiles (in  $c$ -axis projection) do exist. The front and

back profiles are identical, but the orientation of the sawteeth differs for the (110) layer or  $(\bar{1}10)$  layer, which helps differentiate them (to be paralleled with PVCH, for which two orientations of the sawteeth also exist for parts of the crystal in twin relationship).

Finally, to wrap up this analysis of the iPP crystal phases, it is worth emphasizing the major structural difference between the  $\alpha$  and  $\gamma$  phases that precludes considering contact planes parallel to  $\{110\}_{\alpha\text{iPP}}$  for the  $\gamma$  phase (they would be indexed  $\{102\}_{\gamma\text{iPP}}$ ).<sup>6</sup> In  $\gamma$ iPP,<sup>15</sup> the chain axis of half of the helices is oriented nearly at right angles to the  $(100)_{\alpha\text{iPP}}$  plane and therefore would intersect the (110) contact plane also nearly at right angles. Epitaxial crystallization of polymers involves as a rule chains lying with their axis in the contact plane. This is possible for  $\gamma$ iPP only when the contact plane is parallel to the layers made of isochiral helices ( $ac$  for  $\alpha$ iPP,  $ab$  for  $\gamma$ iPP). As already indicated, a contact plane parallel to  $(110)_{\alpha\text{iPP}}$  does not make physical sense for  $\gamma$ iPP since half of the chains in the unit cell would impinge in this contact plane: they would be nearly normal to the plane of the paper in the center parts of Figure 2c. If  $\gamma$ iPP is present and oriented in our samples, this orientation

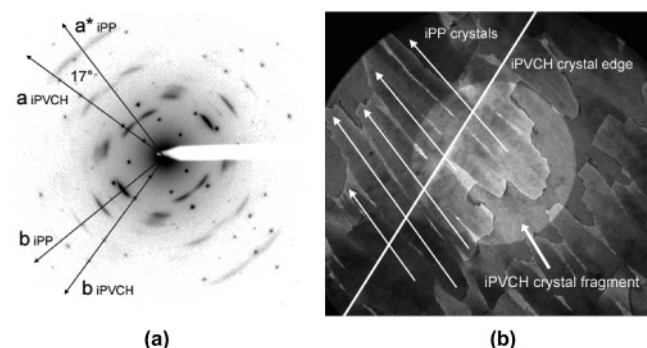


**Figure 3.** (a) Diffraction pattern of a composite PVCH/iPP overgrowth displaying a single orientation of the iPP laths and diffraction pattern. The PVCH single-crystal spots are sharp, and the iPP ones are arced. (b) Corresponding bright-field (actually a defocused diffraction pattern) of the overgrowth of iPP on the lateral faces of single crystals of PVCH. Note the single orientation of the single crystals (parallel thin arrows) at  $17^\circ$  to the PVCH crystal edge normal (indicated with a thick arrow). In both Figures 3 and 6, only part of the PVCH was detached from the glass slide when using the poly(acrylic acid) backing.

results from a “secondary” and later  $\gamma$ iPP/ $\alpha$ iPP epitaxy on  $\alpha$ iPP crystals oriented through an initial  $\alpha$ iPP/PVCH epitaxy.<sup>6,9</sup>

## Experimental Results and Analysis

### 1. Epitaxy of iPP on Untwinned Single Crystals of PVCH

**Form I: Evidence for a Dimensional and Topographical Match.** As indicated in the Introduction, the conventional experimental procedure developed in this laboratory is to use various epitaxial crystallizations in succession to investigate polymer/polymer interactions.<sup>1</sup> First, the (future) substrate polymer is crystallized epitaxially on a low-molecular-weight (MW) organic compound (e.g., benzoic acid or its salts). After washing away the low-MW compound, this initial step yields a polymeric substrate in which the chain axis lies in the plane of the film. Well-defined ( $hk0$ ) planes are thus exposed—they may be of different type or even of different crystal polymorphs depending on the substrate used. The second polymer, of lower melting point, is then deposited on this substrate, melted, and recrystallized. A bilayer polymer film is obtained that yields a composite diffraction pattern from which the two contact planes and relative chain orientations can be deduced.<sup>1</sup> In essence, however, the whole analysis rests on the observation of polymers that are oriented with their chains at right angles to the electron beam.

In the present investigation of the PVCH/iPP structural relationship, one piece of information is available: namely, when the two polymers are cocrystallized in a fiber form, the chain axes of the two polymers are parallel. This implies a very reasonable and expected matching of the two chain axis repeat distances that are indeed virtually equal despite the different helix conformations.

Assuming that this dimensional match is involved in the structural relationship, the main concern then shifts to investigating the lateral organization of the chains in the contact plane. For this purpose, investigation of single crystals is most appropriate since electron diffraction visualizes the two polymers along their axis, that is, helps determine the organization of the stems in the epitaxial relationship. This option has been used in the present case. It turns out to yield a wealth of information.

Figure 3 shows the overgrowth of iPP single crystals on the lateral edges of PVCH crystals and the corresponding diffraction pattern. The iPP laths are elongated in the  $a^*$  direction of the  $\alpha$  phase and display frequently thicker edges (Figure 3b). These edges result from the epitaxial crystallization of  $\gamma$ iPP phase on

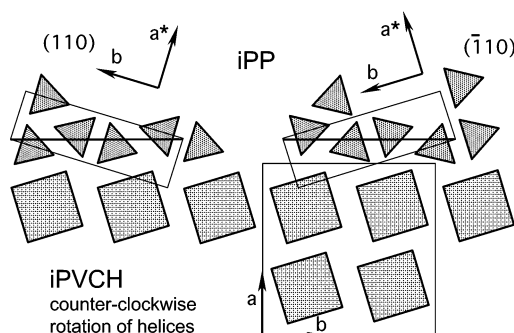


**Figure 4.** Possible epitaxial interactions between  $\alpha$ iPP and PVCH based on the geometrical matching of the two lattices: both (110) and ( $\bar{1}10$ )  $\alpha$ iPP contact planes may be considered.

the single crystals of  $\alpha$ iPP.<sup>14</sup> Strikingly, the laths of  $\alpha$ iPP are systematically oriented at a constant angle ( $\approx 17^\circ$ ) to the PVCH crystal edge normal. The composite diffraction pattern made of the  $hk0_{\alpha\text{iPP}}$  and  $hk0_{\text{PVCH}}$  patterns is shown in Figure 3a. Analysis of this composite pattern helps establish at once (a) the geometrical and (b) the structural match at the root of the  $\alpha$ iPP/PVCH epitaxial relationship.

(a) The geometrical match stems from the observation that one  $110_{\alpha\text{iPP}}$  reflection is aligned with the 200 reflection of PVCH, which suggests that the  $(110)_{\alpha\text{iPP}}$  plane and  $(200)_{\text{PVCH}}$  (i.e.,  $(100)_{\text{PVCH}}$ ) plane are contact planes in the epitaxy. The dimensional match associated with these contact planes is straightforward. The  $a$  parameter of the PVCH unit cell is 21.99 Å. The repeat distance along the  $(110)_{\alpha\text{iPP}}$  plane and normal to the iPP chain axis is 21.96 Å and matches almost perfectly this distance (in both cases, using room temperature cell dimensions) (Figure 4). Combined with the matching of  $c$ -axis parameters (both  $\approx 6.5$  Å), we are therefore dealing with a nearly perfect two-dimensional lattice match. Note, however, that the  $(110)$  contact face of iPP displays a slightly monoclinic geometry with an angle of  $\approx 93^\circ$  (Figure 2c). Disregarding this slight monoclinicity, we are dealing in the present case with a two-dimensional lattice match. This is a rare situation in the field of polymer epitaxy, in which one-dimensional match is more common.<sup>1</sup>

Considering only the parallelism and dimensional matching, two possibilities would still need to be considered, as shown schematically in Figure 4: the  $\alpha$ iPP contact plane could be  $(110)$  or  $(\bar{1}10)$ . Fortunately, the diffraction pattern of Figure 3a provides more detailed information on the epitaxial relationship.

(b) The structural relationship is more involved. Beyond the parallelism of  $\{110\}_{\alpha\text{iPP}}$  and  $(100)_{\text{PVCH}}$  planes, Figure 3a provides additional essential information. It indicates that there is a strict relationship between the PVCH  $hk0$  pattern “asymmetry” (or handedness) and the orientation of the  $\alpha$ iPP epitaxial overgrowths. With the help of the detailed structural analysis of the two crystal structures and contact plane topographies developed earlier, it is possible to work out this relationship. Specifically, this diffraction pattern indicates that when the PVCH helices are rotated counterclockwise relative to the PVCH cell edges, the  $\alpha$ iPP contact plane is  $(110)$ . This information, in turn, indicates that the major feature at play is the “asymmetric sawteeth” topography of the contact planes, when seen along the common chain axis orientation. Both  $\alpha$ iPP and PVCH contact planes display this asymmetric surface topography. In other words, the profiles of the asymmetric sawteeth patterns match in the PVCH and  $\alpha$ iPP contact planes. More precisely, when the PVCH helices are rotated counterclockwise, the contact plane is  $(110)_{\alpha\text{iPP}}$  rather than  $(\bar{1}10)_{\alpha\text{iPP}}$ . In Figure 4, the left-hand-side model is therefore the only valid option.

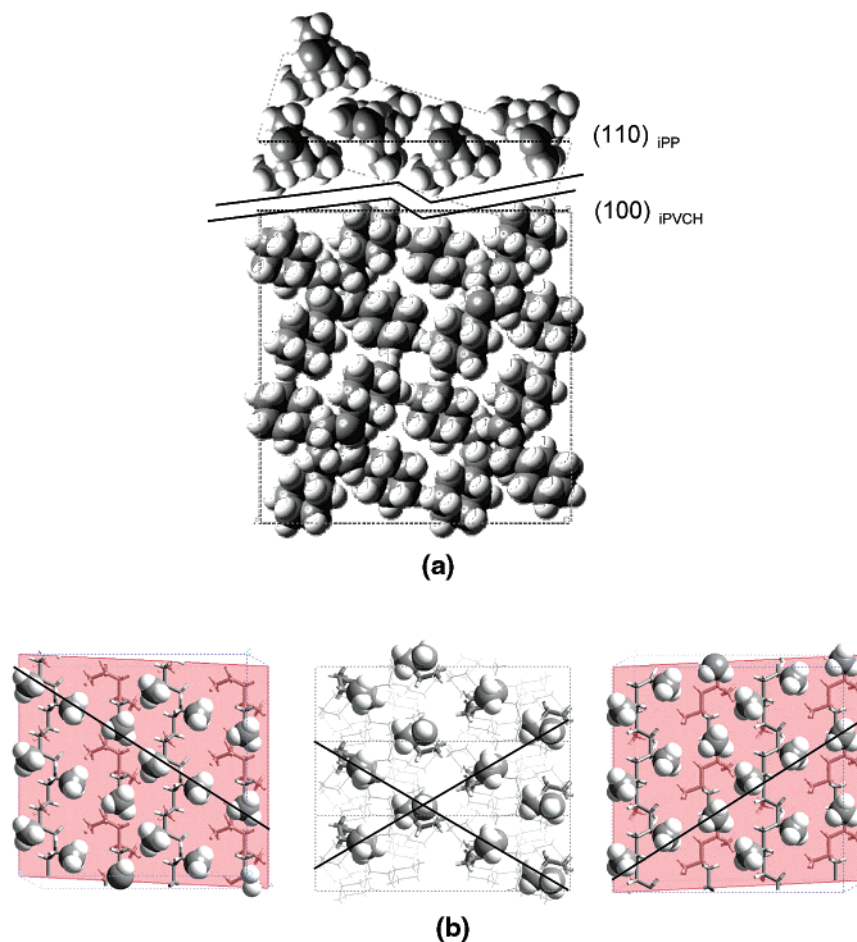


**Figure 5.** iPP/PVCH interactions in the contact plane. (a) Space-filling molecular model of the interactions as seen along the chain axis direction: the asymmetric sawtooth profiles of iPP and PVCH match. (b) Molecular models of the contact faces. The center represents the PVCH (100) contact face. On both sides, the matching front and back faces of the (110) layer are chiral, with rows of methyl groups symmetrically tilted at  $\pm 57^\circ$  to the chain axis. Folding of these iPP faces on top of the PVCH contact face (like iPP shutters closing a PVCH window) results in the alignment of the methyl rows with either one or the other rows of edges of the cyclohexyl rings, also tilted at  $57^\circ$  to the chain axis.

The structural analysis arrived at is also consistent with the fact that, as developed earlier, the contact face of PVCH is racemic from conformational and topographical standpoints: right- and left-handed helices are present in the face. The  $\alpha$ iPP contact faces are not racemic since in any one face, helices of one hand are more exposed than helices of the other hand. However, as shown in Figure 2c, opposite sides of the same layer are mirror images, although they share the same  $a$ -axis orientation. Either the front face or the back face of a (110) $_{\alpha$ iPP layer can become contact planes on a given PVCH contact face. They generate the same orientation of the  $a^*$  axis relative to the PVCH contact face.

The PVCH/iPP structural matching is best illustrated with the space-filling models in Figure 5. Figure 5a shows the interactions along the  $c$  axis. This representation is valid for both the front and back faces of the (110) layer (when considering only the projections of the helices). The contact faces are shown in Figure 5b. Interaction of these iPP faces with the PVCH face (center) results in the alignment of the iPP methyl rows with the cyclohexyl rings edges. Since the PVCH face is racemic, the two chiral iPP faces shown are equally suited to become contact planes.<sup>19</sup>

To summarize, the epitaxial relationship results from an unusual similarity between the two contact faces involved. The two faces have very similar dimensions (within fractions of an angstrom), and their topographies are so similar that they can match easily. Both contact faces display (i) along the chain axis

direction the “asymmetric sawteeth” with  $\approx 11$  Å periodicity and (ii) at some  $57^\circ$  to the chain axis rows 5.5 Å apart of methyl side groups (iPP) or of the exposed parts of the cyclohexyl side groups (PVCH).

## 2. Epitaxy of iPP on Twinned Single Crystals of PVCH Form I: Epitaxial Growth as a Structural Marker.

The above analysis of the PVCH/iPP epitaxial relationship has been based on the simplest and most straightforward experimental evidence that could be collected. In practice, the situation may be more complex due to a feature of PVCH crystals: they are very frequently growth twins. The structural consequences of this twinning, in relation to iPP epitaxial growth, are worth being presented briefly. Indeed, because of the highly specific interactions at the root of the PVCH/iPP epitaxy, epitaxial growth of  $\alpha$ iPP turns out to provide an original epitaxial marker for the internal structure of PVCH crystals.

Figure 6 shows the diffraction pattern and bright-field image of a more complex PVCH crystal. Two orientations of the  $\alpha$ iPP single crystals are observed, which differ by the clock- or counterclockwise  $17^\circ$  tilt relative to the PVCH face normal. Likewise, the diffraction pattern is a composite of a single PVCH diffraction pattern and of two  $\alpha$ iPP patterns. The two latter patterns share, however, one reflection, which is the superposition of  $110_{iPP1}$  and  $110_{iPP2}$ .

This double orientation of iPP overgrowths is related to a “hidden” feature of the PVCH substrate crystal, namely its twinned structure. In the PVCH twins (twinning by merohedry),



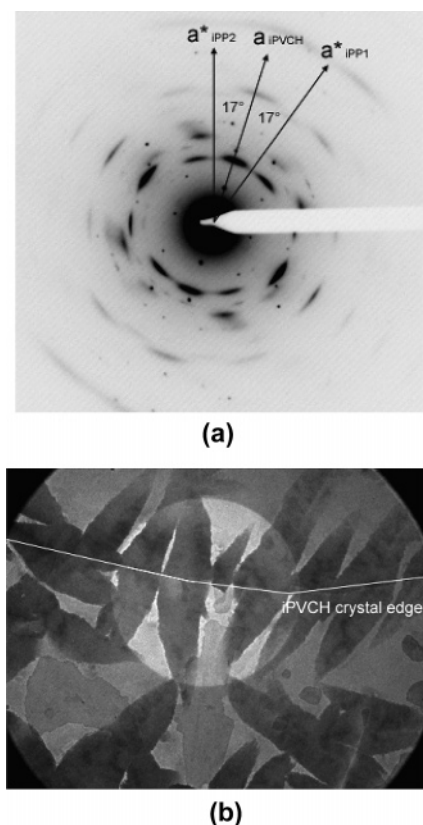
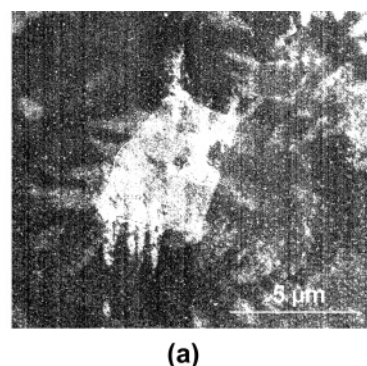


**Figure 6.** (a) A composite PVCH/iPP diffraction pattern displaying two orientations of the iPP overgrowth. The corresponding  $a_{\text{PVCH}}$  and  $a^*_{\text{iPP}}$  axes orientations are indicated. The  $110_{\text{iPP1}}$  and  $110_{\text{iPP2}}$  combine in a single diffraction spot located on the  $a_{\text{PVCH}}$  axis. (b) Corresponding defocused diffraction pattern: overgrowth of iPP on the lateral, top face of a single crystals of PVCH (PVCH crystal fragments appear as small gray islands in the lower part of the figure). Note the two orientations of the elongated  $\alpha\text{iPP}$  single-crystal laths at  $\pm 17^\circ$  to the PVCH crystal edge normal (the  $a^*$  axis of  $\alpha\text{iPP}$  is oriented parallel to the long axis of the lath).

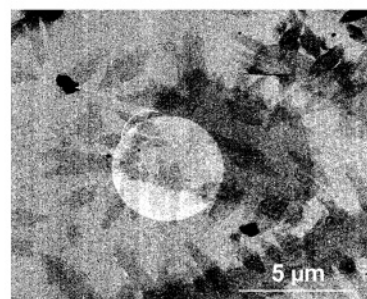
the twin components differ by the azimuthal setting of the helices in the unit cell: they are tilted either clock- or counterclockwise relative to the cell edges. In our previous study,<sup>13</sup> we observed that PVCH crystals grown under similar conditions to the present ones are made of relatively large twinned domains or are even single crystalline, while single crystals grown from solutions in squalane or phenyldecane display a spectacular polysynthetic twinning of the growth sectors.

To show that the two orientations of  $\alpha\text{iPP}$  overgrowths are associated with the twinning of the PVCH crystals, the use of dark-field imaging is most appropriate.

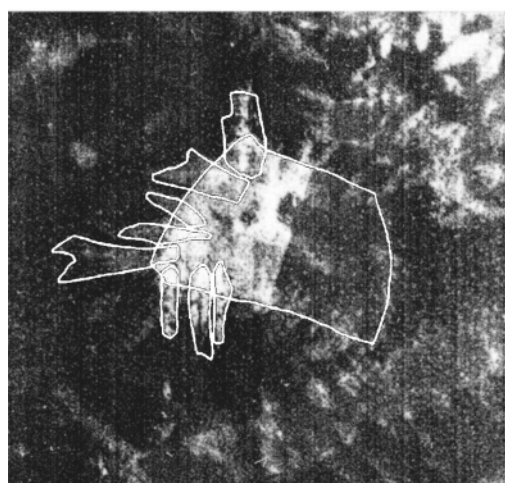
Dark-field imaging was already successfully applied to map the PVCH crystals' twinned domains. In the PVCH crystals, domains with a given azimuthal setting of the helices can be distinguished from those with the twinned, symmetrical setting by imaging the crystal through the overlapped strong  $240_{\text{ccw}}$  and twinned weak  $240_{\text{cw}}$  spots of the diffraction pattern.<sup>13</sup> In the dark-field image, domains imaged through the stronger  $240_{\text{ccw}}$  spot appear brighter than domains imaged through the weaker  $240_{\text{cw}}$  spot. Figure 7 illustrates in detail the above imaging procedure (with explanatory drawings of the corresponding dark-field and diffraction pattern in Figure 8). It displays a large PVCH single crystal that is made of two roughly equal sized twinned parts, with the twin plane oriented at  $\approx$ one o'clock. In this case, the left-hand side of the crystal is imaged through the strong  $240_{\text{cw}}$  reflection, whereas the right-hand part



(a)



(b)



(c)

**Figure 7.** (a) Dark-field imaging of a complex (twinned) PVCH single crystal with its iPP overgrowths. The  $240_{\text{PVCH}}$  diffraction spot and its nearby  $040_{\text{iPP}}$  spot are selected simultaneously (cf. Figure 8a). They image the PVCH crystal parts and corresponding iPP overgrowths (bright domains), whereas the twinned parts of the PVCH and their iPP overgrowths appear darker. (b) Corresponding bright-field image of the crystal in part (a) that helps visualize the twinned part of the crystal that is not imaged in dark-field. (c) Schematic drawing of the crystals shown in (a) that helps locate the twinned components of the PVCH single crystal and associated iPP overgrowths orientations. Only iPP crystals with a single orientation are imaged by this selected area imaging technique, since only one  $040_{\text{iPP}}$  spot is used. The underlined iPP crystals oriented at nine o'clock indicate the same relationship with the PVCH crystal but have grown on its lateral face.

is virtually invisible (imaged through the weaker  $240_{\text{ccw}}$  reflection).

Figure 7 also shows that some (but only some) overgrown iPP laths are imaged in dark-field (in Figure 7a, the spikes oriented at  $\approx$ twelve o'clock). This selectivity is easily understood when considering the composite PVCH/iPP diffraction pattern. In this pattern, the  $040_{\alpha\text{iPP}}$  spot of iPP crystals grown on the  $(100)_{\text{PVCH}}$  face is located near the strong PVCH  $240$  spot (Figure 8a). By selecting both  $040_{\alpha\text{iPP}}$  and the overlapped PVCH

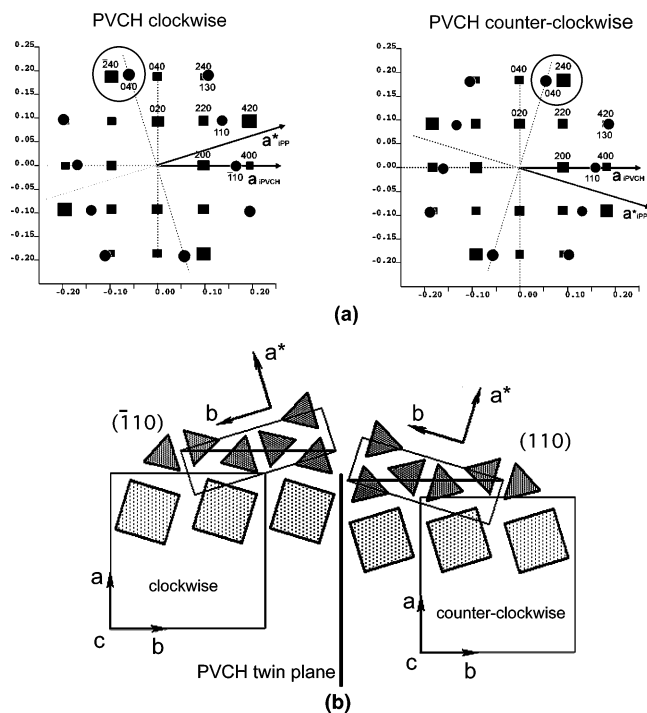


**Figure 8.** (a) Schematic drawing of the possible diffraction patterns of the composite PVCH crystal/iPP overgrowths. The left-hand side illustrates the reflections used for the dark field of Figure 7a,c. The right-hand side pattern would correspond to the twinned component. (b) Molecular and structural interpretation of the diffraction evidence arising from a twinned crystal. The contact layers of iPP on PVCH depend on the azimuthal setting of the PVCH helices, which generates two different orientations of the  $a^*$  axis of iPP overgrowths.

reflections with the objective aperture, the dark-field image highlights only the  $\alpha$ iPP single crystals and those parts of the PVCH single crystals on which the  $\alpha$ iPP single crystals have grown.

A sketch of the composite PVCH/iPP crystals is shown in Figure 7c which illustrates the PVCH crystal edge and the  $\alpha$ iPP overgrowths. Figure 8 regroups the simulated diffraction patterns for the different twinned domains and the  $\alpha$ iPP overgrowth (Figure 8a) as well as the structural interpretation (Figure 8b). They are fully consistent with the structural analyses performed above, extended here to the more realistic case of twinned PVCH crystal substrates.

This investigation of twinned PVCH crystals provides the basis for an unusual epitaxial probe of the internal structure of PVCH crystals. Namely, the orientation of the  $\alpha$ iPP overgrowth depends on, and therefore helps determine, the local clock- or counterclockwise azimuthal rotation of helices in the exposed lateral growth faces of the PVCH crystal (Figure 8b). This information is normally accessible only by dark-field imaging for twinned single crystals of PVCH, as illustrated in our previous work.<sup>13</sup> Morphological probes that help determine such small-scale structural features are quite rare in polymer science. They usually rest on overgrowths of different types: “polymer decoration” (vaporization and condensation/crystallization of e.g. polyethylene) which helps reveal the fold orientation in single crystals,<sup>20</sup> lamellar branching of  $\alpha$ iPP (based on an iPP/iPP homoepitaxy) which helps determine the orientation of the  $a$  axis of the monoclinic unit cell,<sup>4,12</sup> and the above-mentioned epitaxial crystallization of iPP on PTFE which reveals the hand of the iPP helices most exposed in the contact plane.<sup>6</sup> As in the latter case, we are dealing in the present case with a heteroepitaxy, i.e., a morphological marker in which the probe (iPP) differs from the substrate (PVCH). Also, the information

accessed is the PVCH unit-cell inner structure that is not revealed by e.g. the PVCH cell axes’ orientation alone.

It should be noted that similar insights gained through epitaxial relationships, whereas of limited number in polymer science, are not infrequent in mineralogy or materials science since the epitaxial interactions “sense” the substrate structure at a very local scale. Let us recall in this respect that Friedel mentions in his classical textbook (“Leçons de cristallographie”) the very early experiments on epitaxial growth performed by Royer in 1925.<sup>21</sup> Royer observed single orientations of crystals of ammonium iodide epitaxially grown on cleavage surfaces of mica, i.e., discovered through epitaxial crystallization the low symmetry of the mica cleavage plane—although the detailed structural analysis of mica was made only much later.

## Discussion and Conclusion

The  $\alpha$ iPP/PVCH epitaxy provides a clear example of two-dimensional lattice match. The chain axis repeats are nearly identical despite the different helix conformations. Dimensional match in the interhelix direction is ensured by the fact that  $(110)_{\alpha iPP}$  and  $(\bar{1}10)_{\alpha iPP}$  become the contact planes and match within fractions of angstroms the  $a$  parameter of the PVCH unit cell. The setting of the helices in the PVCH contact face determines whether the  $(110)$  or the  $(\bar{1}10)$  layer of  $\alpha$ iPP becomes the contact layer. Single-crystal electron diffraction patterns and dark-field imaging demonstrate that the epitaxial relationship between  $\alpha$ iPP and PVCH results not only from a dimensional matching but also from a topographic matching of the contact faces, namely the common orientation and matching of their “asymmetric sawteeth” surface patterns, associated in PVCH with the tilted setting of the helices.

The structural relationship uncovered in the epitaxial crystallization of  $\alpha$ iPP and isotactic PVCH presents some interesting differences with earlier investigations of epitaxies that involved the  $(110)_{\alpha iPP}$  contact plane. These previous investigations revealed for the most part lattice matching in only one direction, for example matching with the interhelix distance of PTFE. They could nevertheless reveal the helical hand of all the iPP helices involved in the contact plane, mainly because the iPP 5.5 Å periodicity that becomes oriented parallel to the PTFE chain axis materializes the helical path, which differs for right- and left-handed helices. Referring to Figure 2c, epitaxy of iPP on PTFE distinguishes the orientation of methyl groups in the top left and bottom right contact faces from the top-right and bottom-left faces. By contrast, the epitaxy on PVCH distinguishes the top faces from the bottom faces. As a result, the analysis of the helical hands involved in the PVCH/iPP epitaxy cannot be pushed as far, although the dimensional match between PVCH and  $\alpha$ iPP is two-dimensional, which should put more constraints on the topographical match between deposit and substrate. This lack of selectivity stems from the fact that the contact face of PVCH is structurally racemic and from the fact that one matching dimension is along the chain axis of both PVCH and iPP. This in turn fully validates the fact that, in order to establish the structural relationship at the base of the PVCH nucleating activity, we resorted to growth of  $\alpha$ iPP single crystals on PVCH single crystals.

This investigation has also provided a valuable and unexpected outcome. Given the specificity of the molecular interactions (at least in chain axis projection), the orientation of the iPP overgrowth turns out to be a structural marker of the local azimuthal setting of the PVCH helices in the contact plane. This is a welcome addition to the—short—list of epitaxial and



morphological markers that reveal molecular features in polymer science.

## References and Notes

- (1) Wittmann, J. C.; Lotz, B. *Prog. Polym. Sci.* **1990**, *15*, 909.
- (2) Lotz, B.; Thierry, A. *Encycl. Mater. Sci. Technol.* **2001**, 7267. Mathieu, C.; Thierry, A.; Wittmann, J. C.; Lotz, B. *Polymer* **2000**, *41*, 7241.
- (3) Last, A. G. M. *J. Polym. Sci.* **1959**, *11*, 543.
- (4) Lotz, B.; Wittmann, J. C. *J. Polym. Sci., Part B: Polym. Phys.* **1986**, *24*, 1559.
- (5) Lotz, B.; Wittmann, J. C. *J. Polym. Sci., Part B: Polym. Phys.* **1987**, *25*, 1079.
- (6) Yan, S.; Katzenberg, F.; Petermann, J.; Yang, D.; Shen, Y.; Straupé, C.; Wittmann, J. C.; Lotz, B. *Polymer* **2000**, *41*, 2613.
- (7) Mathieu, C.; Thierry, A.; Wittmann, J. C.; Lotz, B. *J. Polym. Sci., Part B: Polym. Phys.* **2002**, *40*, 2504.
- (8) Mitsuishi, K. Polypropylene (Nucleating Agents). In *Polymeric Materials Encyclopedia*; Salamone, J. C., Ed.; CRC Press: Boca Raton, FL, 1996; p 6602.
- (9) Gahleitner, M.; Wolfschwenger, J. Nucleating Agents for Semicrystalline Thermoplastics. *Encycl. Mater. Sci. Technol.* **2001**.
- (10) Kakugo, M.; Wakatsuki, K.; Wakamatsu, K.; Watanabe, K. *Polym. Prepr. (Jpn.)* **1990**, *39*, 3884; *Polym. Prepr. (Jpn.)* **1991**, *40*, 1145.
- (11) Nishikawa, Y.; Murakami, S.; Kohjiya, S.; Kawaguchi, A. *Macromolecules* **1996**, *29*, 5558.
- (12) Lotz, B.; Wittmann, J. C.; Lovinger, A. *J. Polymer* **1996**, *37*, 4979.
- (13) Alcazar, D.; Ruan, J.; Thierry, A.; Kawaguchi, A.; Lotz, B. *Macromolecules* **2006**, *39*, 1008.
- (14) Lotz, B.; Graff, S.; Straupé, C.; Wittmann, J. C. *Polymer* **1991**, *32*, 2902.
- (15) Brückner, S.; Meille, S. V. *Nature (London)* **1989**, *340*, 455.
- (16) De Rosa, C.; Borriello, A. M.; Corradini, P. *Macromolecules* **1996**, *29*, 6323.
- (17) Pradère, P.; Revol, J. F.; Manley, R. St. J. *Macromolecules* **1988**, *21*, 2747.
- (18) We define a chiral face as a face in which topographical features are tilted to the chain axis direction. These features thus mimic the outer path of helices, which helps define "right-handed" and "left-handed" faces or, as is the case with PVCH, racemic faces.
- (19) The interaction between a racemic face (PVCH) and faces of  $\alpha$ iPP that are chiral leads also to a curious situation. The iPP helices that present their "base" in front of the PVCH contact face are all of one hand, yet they interact with helices of PVCH that are alternately right- and left-handed. The interactions in the contact face must therefore be an average between (presumably) more favorable interactions between antichiral and isochiral iPP and PVCH helices. Overall, however, the difference in energy may be limited due to the original organization of the cyclohexyl groups in the PVCH contact face.
- (20) Wittmann, J. C.; Lotz, B. *J. Polym. Sci., Polym. Phys. Ed.* **1985**, *23*, 205.
- (21) Friedel, G. In *Leçons de Cristallographie*; Berger Levraut, Ed.; Paris, 1925.

MA052651R